*Therapeutics, Targets, and Chemical Biology*

Cancer Research

# The Cancer Stem Cell Marker Aldehyde Dehydrogenase Is Required to Maintain a Drug-Tolerant Tumor Cell Subpopulation

Debasish Raha[1], Timothy R. Wilson[1], Jing Peng[2], David Peterson[2], Peng Yue[3], Marie Evangelista[1], Catherine Wilson[1], Mark Merchant[2], and Jeff Settleman[1]

## Abstract

Selective kinase inhibitors have emerged as an important class of cancer therapeutics, and several such drugs are now routinely used to treat advanced-stage disease. However, their clinical benefit is typically short-lived because of the relatively rapid acquisition of drug resistance following treatment response. Accumulating preclinical and clinical data point to a role for a heterogeneous response to treatment within a subpopulation of tumor cells that are intrinsically drug-resistant, such as cancer stem cells. We have previously described an epigenetically determined reversibly drug-tolerant subpopulation of cancer cells that share some properties with cancer stem cells. Here, we define a requirement for the previously established cancer stem cell marker ALDH (aldehyde dehydrogenase) in the maintenance of this drug-tolerant subpopulation. We find that ALDH protects the drug-tolerant subpopulation from the potentially toxic effects of elevated levels of reactive oxygen species (ROS) in these cells, and pharmacologic disruption of ALDH activity leads to accumulation of ROS to toxic levels, consequent DNA damage, and apoptosis specifically within the drug-tolerant subpopulation. Combining ALDH inhibition with other kinase-directed treatments delayed treatment relapse *in vitro* and *in vivo*, revealing a novel combination treatment strategy for cancers that might otherwise rapidly relapse following single-agent therapy. *Cancer Res; 74(13); 3579–90. ©2014 AACR.*

## Introduction

Targeted cancer therapies that exploit the "oncogene addiction" phenomenon observed in many tumor cells can be highly effective in the clinic (1–3). However, responding tumors invariably recur due to acquired drug resistance, probably reflecting the outgrowth of a subpopulation of treatment-refractory cells. The maintenance of many cancers seems to require a subpopulation of tumor cells called cancer stem cells (CSC; ref. 4), which have been identified in hematopoietic and solid malignancies (5), and several studies have described a role for CSCs in drug resistance (6)

Cancer cells are continuously exposed to extrinsic and intrinsic stresses that promote increased reactive oxygen species (ROS) and DNA damage (7–9). The consequent accumulation of mutations in CSCs may render them more vulnerable to stress, especially as they enter S-phase. The activation of DNA damage response (DDR; refs. 10, 11), increased expression of antiapoptotic genes (12), activation of the β-catenin pathway observed in leukemic stem cells (13), and Notch and hedgehog pathways in prostate cancer cells (14) are some of the mechanisms reported to underlie drug resistance in CSCs.

CSCs express various markers, including CD44, CD133, and ALDH1A1, at levels substantially different from the bulk tumor cell population, and these markers are often used to isolate and functionally characterize CSCs. The association of CSC markers such as CD44 and CD133 with drug resistance has thus far been largely based on studies demonstrating reduced sensitivity of CSC marker–positive cells to chemotherapeutic drugs (15) or increased expression of these markers in treatment-resistant tumors (16, 17). There have also been functional roles in drug resistance reported for these markers, including activation of ABC transporters and antiapoptotic genes (18, 19). Elevated ALDH1A1 is observed in CSCs of multiple cancer types (20). ALDH proteins controls the oxidation of aldehydes to corresponding acids, and ALDH-mediated detoxification of toxic aldehyde intermediates produced in cancer cells treated with certain chemotherapy agents has been proposed to confer drug-resistant properties to ALDH1-positive tumor cells (21). Here, we report that cancer cell subpopulations that tolerate otherwise toxic drug exposures express elevated ALDH, which is critical for their survival. Inhibition of ALDH activity effectively eradicates this drug-tolerant subpopulation, revealing a potential beneficial effect of combination therapy that includes ALDH inhibition to delay cancer relapse.

**Authors' Affiliations:** Departments of [1]Discovery Oncology, [2]Translational Oncology, and [3]Bioinformatics, Genentech, Inc., South San Francisco, California

**Note:** Supplementary data for this article are available at Cancer Research Online (http://cancerres.aacrjournals.org/).

**Corresponding Author:** Jeff Settleman, Genentech, Inc., 1 DNA Way, South San Francisco, CA 94080. Phone: 650-467-7140; Fax: 650-225-5770; E-mail: settleman.jeffrey@gene.com

**doi:** 10.1158/0008-5472.CAN-13-3456

## Materials and Methods

### Cell culture

Human cancer cell lines were grown in RPMI media supplemented with sodium pyruvate, 10% FBS, and the antibiotics penicillin and streptomycin at 37°C in 5% $CO_2$. Cell line identity is routinely monitored by SNP-based genotyping in the Genentech cell bank facility.

The Incucyte HD imaging system (Essen BioScience) was used to monitor cell growth in culture, as measured by percentage of confluence. This instrument captures high-definition phase contrast images of cells and uses a contrast based confluence algorithm to compute monolayer confluence of each image over multiple specified time points.

### ALDH activity assays

A bodipy-labeled ALDH substrate (Aldefluor Kit, Stem Cell Technology) was used to detect ALDH activity. The substrate was diluted in RPMI media (5 μL substrate/mL media) and added to adherent cells. After 30 minutes of incubation, cells were washed twice with RPMI media, and microfluorescence images were captured using an IncuCyte HD system (Essen BioScience) with a 10× objective. The quantification of $ALDH^{high}$ cells (∼5% for MKN-45) was based on 16 images captured using the Incucyte System with a 10× objective.

### Flow cytometry

The Aldefluor assay was used to detect ALDH activity in MKN-45 parental cells. $ALDH^{high}$ and $ALDH^{low}$ cells representing about 5% of parental cells with the highest and lowest ALDH activity, respectively, were sorted by flow cytometry. MKN-45 cells incubated with the bodipy-labeled substrate and DEAB, a cold competitive substrate, were compared as a negative control.

### Gene expression analysis

MKN-45 cells were plated on ten 15-cm dishes at $30 \times 10^6$ cells per plate, and grown until 70% confluence and treated with 1 μmol/L crizotinib every 3 days for 4 weeks until drug-tolerant persisters (DTP) were established. Non–drug-treated cells in a 15-cm dish were harvested 3 days after plating. RNA was extracted using a Qiagen RNeasy kit, and RNA was amplified in both parental and DTP cells using the NuGen RNA Amplification Kit. Microarray analysis was carried out in triplicate as previously described (22). Total RNA was isolated from $ALDH^{high}$ and $ALDH^{low}$ cells using a RNeasy column (Qiagen), and microarray-based gene expression analysis was performed on triplicate samples.

### Cell viability assays

Cells were fixed with 4% paraformaldehyde at the end of the assay period, and viability was determined using the nucleic acid stain Syto60 (Life Technologies) diluted 1:5,000 in water (23). Fluorescence was measured using a SpectraMax M5 instrument (excitation 635 nm and emission 695 nm; Molecular Device). Viability was expressed as fraction of a no-treatment control.

### Generation of drug-tolerant cells

MKN-45- and GTL-16–derived DTPs were generated by treating parental cells with 1 μmol/L crizotinib for 15 to 30 days. PC-9 cells were treated with 1 μmol/L erlotinib for 6 to 9 days for DTP generation. Drug concentrations used for DTP generation for all cell lines except GTL-16, EBC-1, and A549 cells are based on previous studies (22). The appropriate concentration of each drug needed for DTP generation was established on the basis of a dose–response curve (Supplementary Table S3). The 200 nmol/L concentration of disulfiram used for most of the cell lines was based on an analysis of disulfiram effects on MKN-45 and GTL-16 DTPs, where an effective cytotoxic disulfiram concentration was empirically determined (Supplementary Fig. S3C). In all cases, media ± drug were changed every 3 days.

### Immunoblotting

Proteins were extracted from cell pellets using NP-40 lysis buffer containing protease and phosphatase inhibitors. Protein concentration was measured using the Pierce BCA protein assay kit. Protein concentrations of samples were derived from a standard curve with BSA. Immunoblots were performed with equal amounts of protein for all samples. This assay generated erroneous concentration values for MKN-45 and GTL-16 DTPs. Therefore, immunoblots of DTP lysates were performed by loading gels with a maximum possible sample volume, and GAPDH levels were measured as a loading control. Proteins were separated using SDS-PAGE and immunodetection was performed using standard protocols. Antibodies were from various vendors: ALDH1A1 (R&D Systems); ALDH1A2 and ALDH8A1 (Santa Cruz Biotechnology); ALDH1A3, ALDH3A1, and phospho-EGFR (Abcam); GAPDH, cleaved PARP, and phospho-ATM/ATR substrates (Cell Signaling Technology); GAPDH (Pierce); and phospho-γH2A.x (Millipore).

### Gene knockdown studies

shRNA constructs were obtained from Sigma-Aldrich. Lentivirus production was carried out in 293T cells as previously described (23). For knockdown studies, GTL-16 cells were plated in 10-cm dishes ($2 \times 10^6$ cells per plate). Following adherence overnight, cells were infected with lentivirus or control virus in the presence of polybrene (Sigma-Aldrich) overnight. Forty-eight hours after infection, cells were re-plated, and following adherence overnight, cells were treated as described above and cell viability was assayed using the Syto 60 nucleic acid stain (LifeTechnologies).

Notably, we were unable to develop suitable transfection and lentivirus infection conditions for MKN-45 cells. Attempts to infect MKN-45 cells with lentiviruses, including the control GFP shRNA virus, resulted in cell death. Attempts to transfect MKN-45 cells with siRNAs using various transfection reagents also failed because of the unusually poor transfection efficiency of this cell line.

### Quantitative PCR analysis

RNA was extracted from parental cells and DTPs using the RNeasy kit and 1 μg RNA was reverse transcribed using the high capacity RNA-to-cDNA Kit (Applied Biosystems). The amount

of amplicon was determined using the Applied Biosystems 7500 quantitative PCR system using SYBR green as the fluorescence reporter and normalized to GAPDH. All samples were analyzed in triplicate and $C_t$ values were determined.

### ROS assays

ROS measurement was performed by flow cytometry. The ROS detection reagent H2DCFH-DA (Molecular Probes) was added to cells in growth media (final concentration: 5 μmol/L), and after 30 minutes at 37°C, cells were harvested. FACS analysis was performed on 10,000 cells per sample. Parental cells not exposed to H2DCFH-DA served as negative control. ROS measurements from parental cells were used to normalize ROS levels for drug-treated cells.

### Xenograft tumor studies

PC-9 cells were suspended in a 1:1 mixture of Hank's Balanced Salt Solution with Matrigel [growth factor–reduced; catalog #356231 (BD Biosciences)] to a final concentration of $5 \times 10^7$ cells/mL. Nude (*nu*/*nu*) mice (Charles River Laboratories) were inoculated subcutaneously with $5 \times 10^6$ PC-9 cells in 100 μL in the dorsal right flank. When tumor volumes reach about 100 to 200 $mm^3$, mice were separated into groups of 10 or 15 animals with similarly sized tumors, and treatment was initiated the following day. Mice were dosed via daily (qd) oral gavage (*per os*) with erlotinib (50 mg/kg in 7.5% captisol) and/or disulfiram (Sigma; Tetraethylthiuram, Catalog # 86720, dosed at 200 mg/kg formulated in safflower oil 95%, benzyl alcohol 5%), or with vehicle only. Tumor volumes were determined using digital calipers (Fred V. Fowler Company, Inc.) using the formula $(L \times W \times W)/2$. Tumor growth inhibition (%TGI) was calculated as percentage of the area under the fitted curve (AUC) for the respective dose group per day in relation to the vehicle: $\%TGI = 100 \times 1 - (\text{AUC treatment/day})/(\text{AUC vehicle/day})$. Curve fitting was applied to $\log_2$-transformed individual tumor volume data using a linear mixed-effects model using the R package nlme, version 3.1–97 in R v2.12.0 (24, 25). Mean time to tumor progression (TTP) was measured as the time (days) to reach twice (2×) or 5 times (5×) initial tumor volume. Partial regressions (PR) are defined as greater than or equal to a 50% decrease from initial tumor volume, and complete regression (CR) is defined as a 100% decrease in tumor volume. Plots were generated and statistical analysis was run using GraphPad Prism 6 (GraphPad Software).

### Metabolic assays

Approximately 5,000 parental cells and 15,000 DTPs were plated per well in XF 96-well microplates (SeahorseBioscience) and incubated for 24 hours at 37°C in 5% $CO_2$. Disulfiram and *N*-acetyl cysteine (NAC) treatments were done for 48 hours in the presence of kinase inhibitor. Oxygen consumption rate (OCR) and extracellular acidification rate (ECAR) measurements were performed in bicarbonate-free, serum-free, 37°C media. Cells were then fixed with 4% paraformaldehyde, stained with Hoechst, and four quadrants/well were imaged using a Molecular Devices ImageXpress HCS. Average nuclei number per quadrant was determined. Bar graphs represented the mean ± SEM of normalized (cell number) OCR and ECAR measurements from six wells.

## Results

### Drug-tolerant cancer cells express the CSC marker ALDH1A1

To identify gene expression differences in the drug-tolerant subpopulation, we analyzed the *MET*-amplified gastric cancer cell line, MKN-45, before and after treatment with the MET kinase inhibitor crizotinib, to which these cells are highly sensitive (Fig. 1A). Following several days of treatment, about 5% of the cells remain viable and largely quiescent indefinitely in continuous crizotinib. Among the gene expression differences (Supplementary Table S1), *ALDH1A1*, one of several ALDH isoforms, was relatively highly expressed in the drug-tolerant subpopulation. Therefore, we further investigated ALDH activity in MKN-45 cells and in a second *MET*-amplified gastric carcinoma cell line, GTL-16.

The ALDH substrate Aldefluor was used to detect ALDH activity in individual cells. We observed clear heterogeneity in ALDH activity within untreated MKN-45 and GTL-16 cell populations, even though they were derived from single cell clones. About 5% of MKN-45 cells expressed detectable ALDH activity ($ALDH^{high)}$) before treatment. Following several days of crizotinib treatment, $ALDH^{high}$ MKN-45 cells were clearly enriched among those that remained viable DTPs (Fig. 1B), and after 30 days, most DTPs were Aldefluor-positive (Supplementary Fig. S1A). Similar findings were made in GTL-16 cells (Supplementary Fig. S1B). These results indicate significant overlap between the Aldefluor-positive and the drug-tolerant subpopulations.

To confirm that the $ALDH^{high}$ cells present before treatment correspond to the drug-tolerant population, we used two approaches. First, viability of MKN-45 $ALDH^{high}$ and $ALDH^{low}$ cells, separated by fluorescence-activated cell sorting (FACS; Supplementary Fig. S2A), was measured following 72-hour crizotinib treatment. The second assay involved treating $ALDH^{high}$ and $ALDH^{low}$ cells with crizotinib for 3 weeks and then allowing DTPs to expand as colonies in the absence of drug. Both assays revealed increased crizotinib tolerance by MKN-45 $ALDH^{high}$ cells compared with $ALDH^{low}$ cells (Supplementary Fig. S2B), whereas there was no difference in growth rates of $ALDH^{high}$ and $ALDH^{low}$ cells (Supplementary Fig. S2C). $ALDH^{high}$ cells yielded more colonies of larger size (Supplementary Fig. S2D), and $ALDH^{high}$-derived colonies consist of both $ALDH^{high}$ and $ALDH^{low}$ cells, indicating that $ALDH^{high}$ cells can give rise to $ALDH^{low}$ cells (Supplementary Fig. S2E).

Although Aldefluor is the preferred substrate for the ALDH1A1 isoform (26), Aldefluor can be converted by other ALDH isoforms (27). To determine which ALDH family member(s) contribute to increased ALDH activity in $ALDH^{high}$ cells, we FACS-sorted MKN-45 cells into $ALDH^{high}$ and $ALDH^{low}$ cells and observed about 8-fold upregulation of *ALDH1A1* levels in $ALDH^{high}$ cells but no significant expression difference for 18 other ALDH isoforms (Supplementary Fig. S1C). Similarly, ALDH1A1 protein expression was higher in $ALDH^{high}$ cells (Fig. 1C). Increased ALDH1A1 was also observed in crizotinib-treated MKN-45 within 24 hours (Fig. 1D) before drug-induced

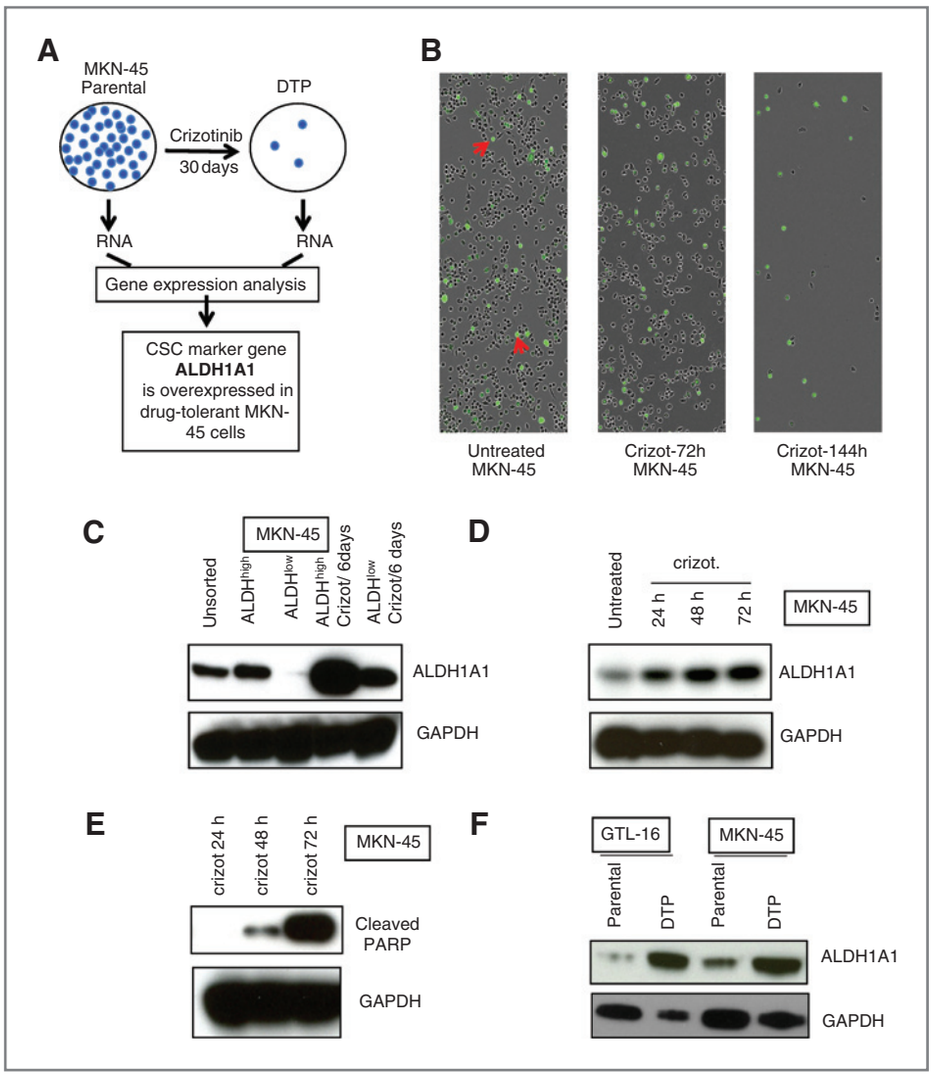


**Figure 1.** Drug-tolerant gastric cancer cells express relatively high levels of *ALDH1A1*. A, gene expression analysis of MKN-45 parental and crizotinib-tolerant cells revealed *ALDH1A1* as one of the most differentially expressed genes. B, ALDH activity (green) was measured in MKN-45 parental and crizotinib-tolerant cells using Aldefluor. Red arrows, examples of ALDH$^{high}$ cells in the parental population. C, immunoblots illustrating higher basal and crizotinib-induced ALDH1A1 protein in ALDH$^{high}$ cells compared with ALDH$^{low}$ cells. D, immunoblots demonstrating kinetics of ALDH1A1 induction in crizotinib-treated MKN-45 cells. E, immunoblots illustrating induction of ALDH1A1 in crizotinib-treated MKN-45 cells before apoptosis, measured as cleaved PARP. F, immunoblots illustrating elevated ALDH1A1 in MKN-45- and GTL-16–derived DTPs.

apoptosis was detected (Fig. 1E). ALDH1A1 protein was induced in ALDH$^{high}$ and ALDH$^{low}$ MKN-45 cells, albeit at much lower levels in ALDH$^{low}$ cells (Fig. 1C). Consistent with the enrichment of ALDH$^{high}$ cells in the drug-tolerant subpopulation, increased ALDH1A1 was observed in MKN-45 and GTL-16 DTPs (Fig. 1F). These results indicate that ALDH$^{high}$ cells, present before treatment, and crizotinib-tolerant DTPs are largely overlapping populations, both expressing elevated ALDH1A1.

### ALDH is required by drug-tolerant cancer cells

To examine a functional role for ALDH in drug tolerance, we used the drug disulfiram, which irreversibly inhibits ALDH enzymatic activity (28, 29). Disulfiram-treated MKN-45 and GTL-16 cells exhibited no significant viability effects (Supplementary Fig. S3), but when combined with crizotinib, disulfiram potently eliminated crizotinib-tolerant MKN-45 and GTL-16 cells (Fig. 2A and B). Although a brief preexposure to disulfiram modestly reduced DTPs for some cell lines, it did not eliminate all DTPs, indicating that continuous disulfiram exposure is required to substantially reduce the drug-tolerant subpopulation (Supplementary Fig. S4A). When MKN-45- and GTL-16-derived DTPs, established by treatment with crizotinib, were subsequently exposed to disulfiram, they were effectively eliminated (Supplementary Fig. S4B), confirming a critical requirement for ALDH for DTP survival. Multiple ALDH isoforms are increased in GTL-16 DTPs (Supplementary Fig. S5A and S5B), and knockdown of *ALDH1A1* had no effect on drug sensitivity or DTP formation (Supplementary Fig. S6A and S6B), implicating additional ALDH enzymes. Although we were unable to knockdown ALDH1A1 in MKN-45 cells for technical reasons, expression of 12/19 ALDH isoforms was detected in MKN-45 parental cells and DTPs (Supplementary Fig. S5D), implicating potential redundancy.

We also tested disulfiram with the ALDH1A1-negative *EGFR*-mutant lung carcinoma cell line PC-9 (Supplementary Fig. S5C), which expresses other ALDH isoforms (Supplementary Fig. S5A and S5B). PC-9 cells are EGFR-addicted and very

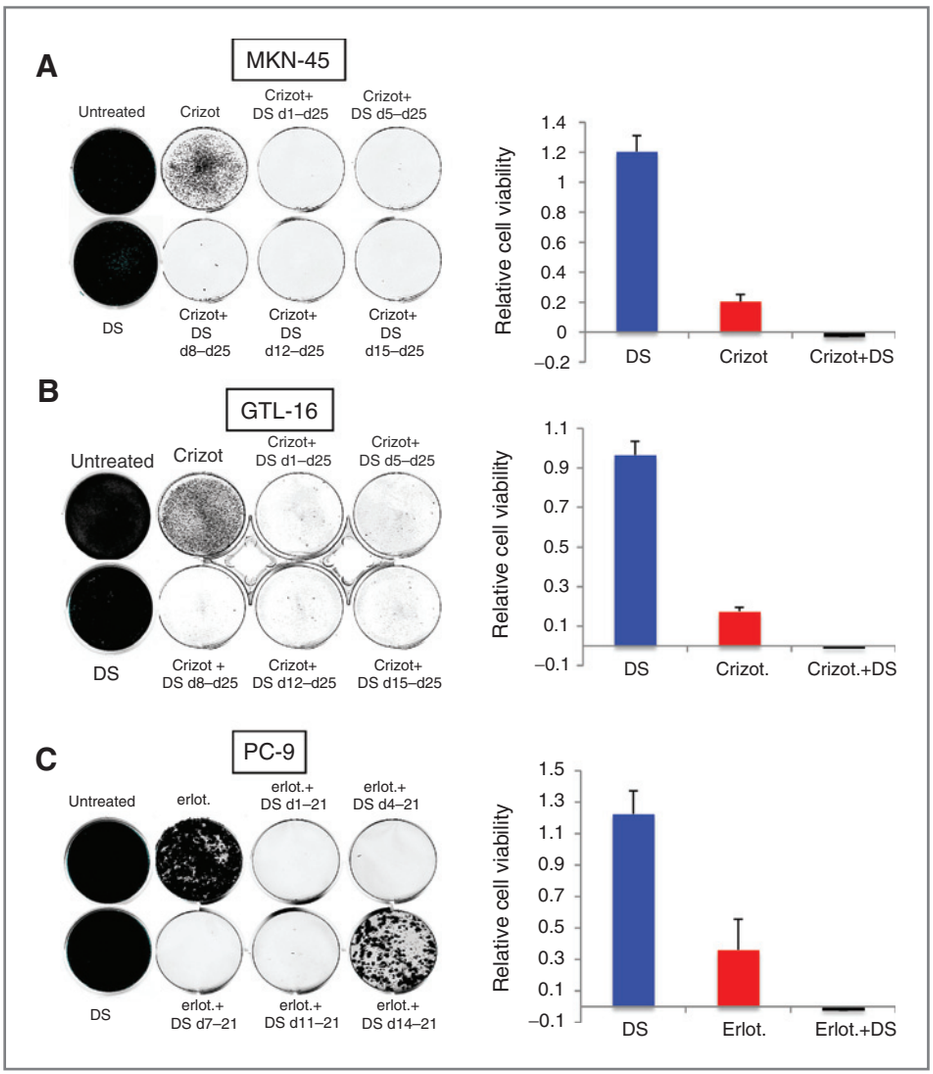


**Figure 2.** The ALDH inhibitor disulfiram eliminates drug-tolerant cells. MKN-45 (A) and GTL-16 (B) cells were treated with 1 μmol/L crizotinib for 25 days (d1–d25) and 200 nmol/L disulfiram (DS) was added either on d1 along with crizotinib or at later time points (d5, d8, d12, and d15), and treatment was continued until d25. C, parental PC-9 cells were treated with 1 μmol/L erlotinib for 21 days (d1–d21) and 200 nmol/L disulfiram was added at several time points (d1, d4, d7, d11, and d14) during erlotinib treatment, and the treatment continued until d21. Cell viability was determined using the Syto60 assay. Bar graphs represent quantitative measurements of the lethal effect of disulfiram on drug-tolerant cells as measured by Syto60 viability assay after treatment for 15 days for MKN-45 and GTL-16 cells and 10 days for PC-9 cells. Cell viability from triplicate wells is expressed as a fraction of untreated control. The error bars reflect SEM values. DS, disulfiram.

sensitive to treatment with the EGFR inhibitor erlotinib (22). Disulfiram plus erlotinib effectively killed erlotinib-tolerant PC-9 cells (Fig. 2C). PC-9–derived DTPs begin expanding as colonies when treated with erlotinib beyond 10 days (Supplementary Fig. S3A and S3B) while maintaining drug tolerance. We previously described these expanded clones as drug-tolerant expanded persisters (22), which, unlike DTPs, are relatively refractory to disulfiram (Fig. 2C). Consistent with the observed effects of disulfiram on PC-9–derived DTPs, expression of several ALDH family members was increased (Supplementary Fig. S5A and S5B). These results implicate multiple ALDH family members in drug tolerance and suggest that the role for ALDH in maintaining the viability of this subpopulation is most critical before their expansion as drug-tolerant clones.

We extended these findings to additional kinase-dependent cancer cells. In eight cancer cell lines derived from breast, colon, and lung tumors, with previously established kinase dependency, combining disulfiram with kinase inhibition substantially reduced drug-tolerant clones (Fig. 3A and B). Disulfiram alone did not cause significant cell death in any tested cell lines.

A similar effect of disulfiram was observed on DTPs derived from treating GTL-16 cells with the DNA-damaging agent, etoposide (Supplementary Fig. S4C). Gossypol, another ALDH inhibitor (30), also showed effectiveness, although with less potency than disulfiram, in killing drug-tolerant cells (Supplementary Fig. S7A). To exclude the possibility that the cytotoxic effect of disulfiram reflects activity on low-density cultures (DTPs), we plated GTL-16 cells and DTPs at different densities and treated with disulfiram. Irrespective of plating density, disulfiram effectively killed most DTPs, whereas no cytotoxic effect was observed on parental cells plated at the same densities (Supplementary Fig. S6C). A similar analysis of PC-9 parental cells revealed disulfiram sensitivity only in DTPs (Supplementary Fig. S6D). These results collectively support the potentially broad ALDH requirement in a drug-tolerant subpopulation of cancer cells.

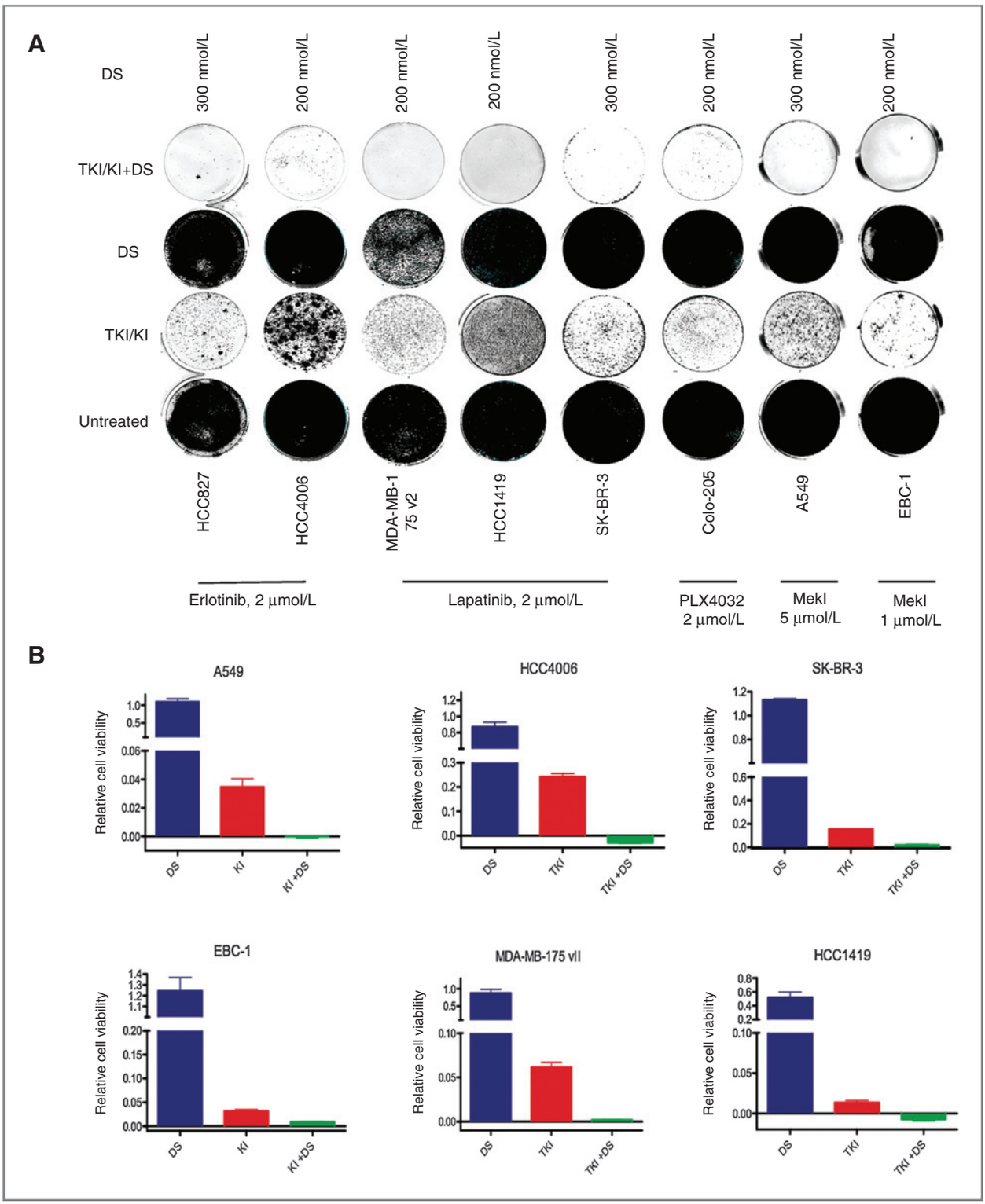


Figure 3. Drug-tolerant cancer cells of various tissue origins are sensitive to disulfiram. A, the lethal effect of disulfiram (DS) and kinase inhibitor (KI) combinations on cancer cells addicted to various oncogenes. The cancer cell lines sensitive to erlotinib (HCC827 and HCC4006), lapatinib (HCC1419, SKBR3, and MDA-MB-175 v2), MEK inhibitor AS703026 (A549 and EBC-1), or BRAF inhibitor PLX0432 (Colo-205) were treated with the appropriate kinase inhibitors, either alone or in combination with 200 to 300 nmol/L disulfiram. The duration of treatment varied from 11 to 25 days depending on the time it took for the combination treatment to kill most of the drug-tolerant cells. B, the bar graphs represent quantitative measurements (triplicate wells per treatment) of the disulfiram effect on cell viability as measured by the Syto60 assay and expressed as a fraction of the untreated control. The error bars reflect SEM values. DS, disulfiram.

**The drug-tolerant subpopulation experiences increased oxidative stress**

The ALDH requirement in drug-tolerant cells might reflect increased levels of toxic aldehydes, resulting from peroxidation of membrane lipids (31), due to oxidative stress associated with increased ROS. The drug-resistant properties of CSCs may reflect, in part, the activation of adaptive responses to continuous exposure to low level stress (32), often associated with increased ROS and a DDR (33). Because mitochondria are the major source of ROS, we examined the bioenergetics of ALDH$^{high}$ cancer cells by measuring their OCR, an indicator of mitochondrial electron transport chain (ETC) activity, and their ECAR, an indicator of glycolytic activity. Although the extent of energy production through the glycolytic pathway is

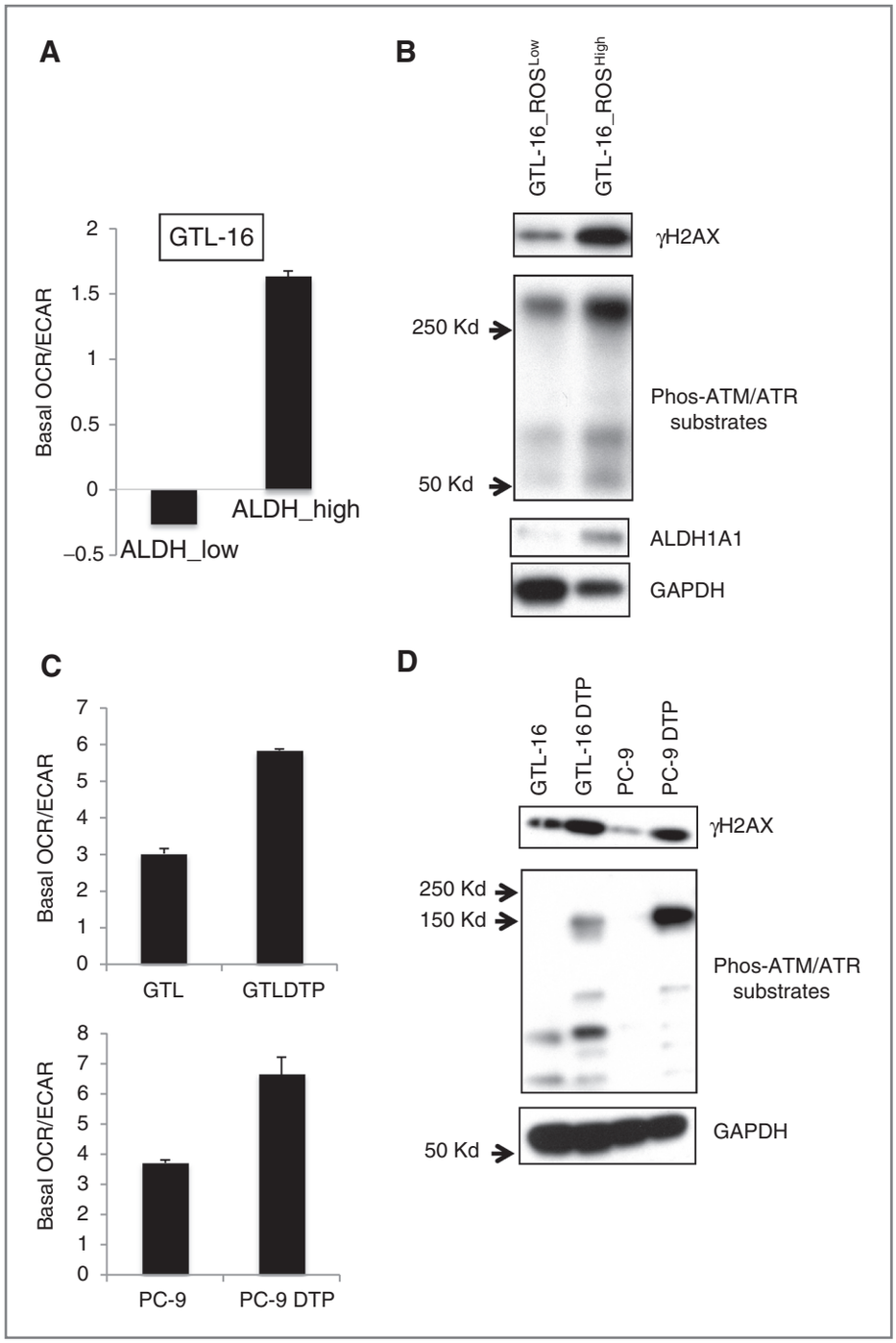


Figure 4. Similar mitochondrial activity and DDR in ALDH$^{high}$ and drug-tolerant cells. A, OCR and ECAR, reflective of energy production by mitochondrial respiration and glycolysis, respectively, were measured using a Seahorse XF 96 in ALDH$^{high}$ and ALDH$^{low}$ GTL-16 cells sorted by flow cytometry. B, immunoblots illustrating increased expression level of the DNA damage sensor phospho-γH2A.x and phospho-ATM/ATR substrates in ALDH$^{high}$ cells. C, OCR and ECAR analyses performed on GTL-16 DTPs treated with 1 μmol/L crizotinib for 15 days and PC-9 DTPs treated with 1 μmol/L erlotinib for 7 days reveal mitochondrial respiration as the main source of energy production in DTPs. D, immunoblot data indicating increased DNA damage and activation of a DDR in DTPs.

similar between GTL-16 ALDH$^{high}$ and ALDH$^{low}$ cells, the basal OCR in ALDH$^{high}$ cells is significantly higher (Fig. 4A and Supplementary Fig. S8A). These results reveal increased mitochondrial respiration in ALDH$^{high}$ cells, which might lead to increased ROS. Indeed, we detected relatively high ROS levels (ROS$^{high}$) in ALDH$^{high}$ cells (Supplementary Fig. S8C). We then sorted cells based on ROS levels and measured ALDH1A1 (Fig. 4B and Supplementary Fig. S8B). Consistent with flow cytometric results, ROS$^{high}$ cells expressed higher ALDH1A1 than ROS$^{low}$ cells. Increased DNA damage, a consequence of increased ROS, was also observed in ROS$^{high}$ cells, measured as increased phospho-γH2A.x and phospho-substrates of ATM/ATR, indicators of double-stranded DNA breaks and DDR, respectively (Fig. 4B and Supplementary Fig. S8B). Both indicators were higher in ROS$^{high}$ cells, further supporting the CSC-like properties of ALDH$^{high}$ cells. Furthermore, as in ALDH$^{high}$ cells, DTPs exhibit increased dependence on mitochondrial respiration (Fig. 4C), suggesting elevated oxidative stress in DTPs. Increased DNA damage sensor and transducer activity was also observed in DTPs (Fig. 4D). These results suggest that

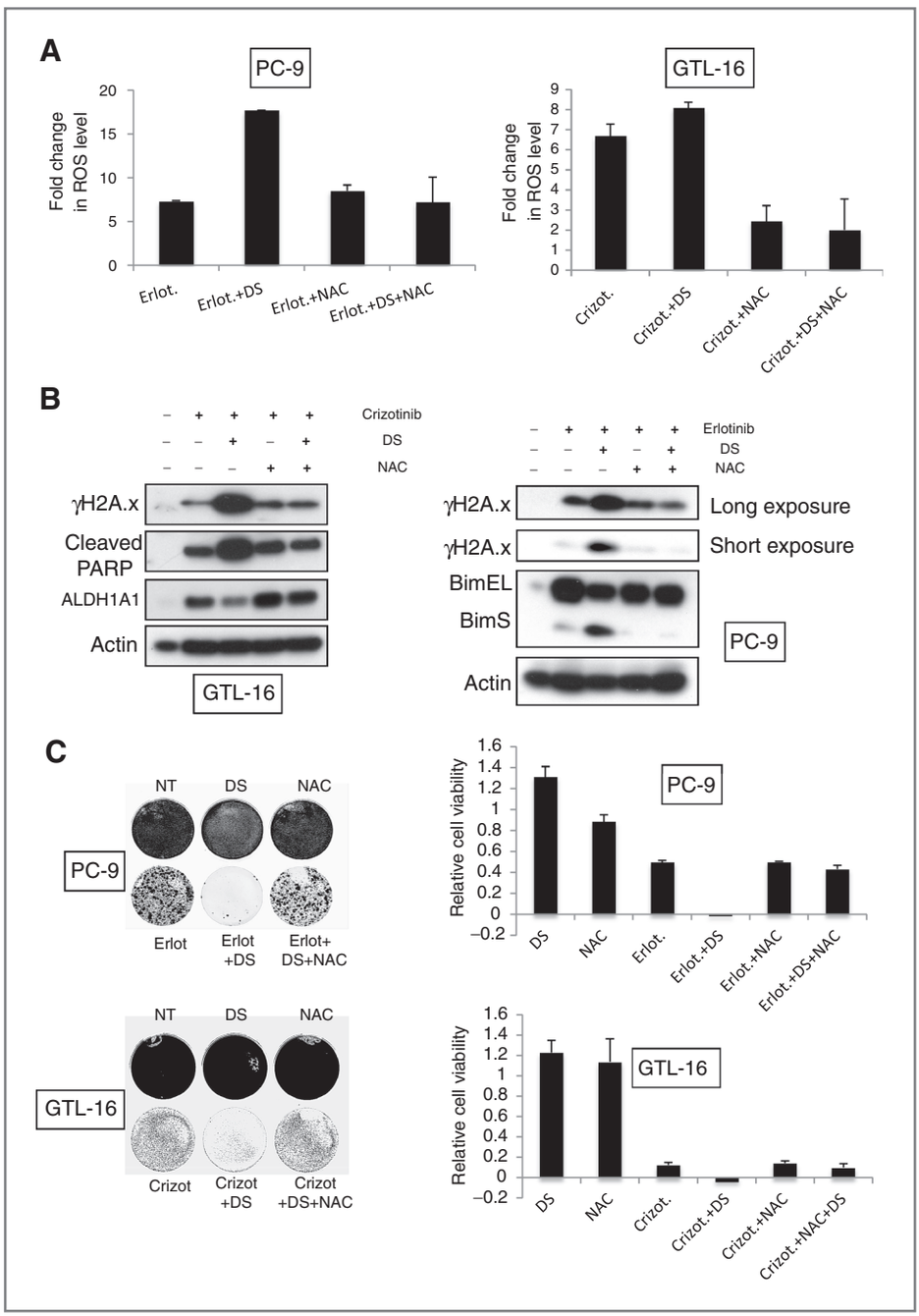


**Figure 5.** ALDH functions as a ROS regulator. A, ROS levels were detected using the fluorescein-based H2DCFH-DA reagent and measured by flow cytometry. PC-9 and GTL-16 cells were treated with erlotinib and crizotinib for 8 and 15 days, respectively. DTPs were exposed to disulfiram (DS; 200 nmol/L) and NAC (5 mmol/L) for 48 hours during kinase inhibitor treatment. The bar graphs represent the fold change in ROS levels for each treatment (three replicates) compared with untreated parental cells. B, immunoblot data demonstrate a disulfiram-induced increase in double-stranded DNA breaks (phospho-γH2A.x; long and short exposures of the same immunoblot are shown) and apoptosis, as measured by cleaved PARP and BimS levels in DTPs, and reversal of these effects in the presence of the ROS scavenger NAC. C, PC-9 and GTL-16 cells were treated with erlotinib and crizotinib, respectively, either alone or in combination with disulfiram and NAC. Cell viability was determined after 10 days of treatment for PC-9 cells and 17 days for GTL-16 cells by the Syto60 assay. Bar graphs represent quantitative measurements of the effect of each treatment from three replicates, expressed as cell viability relative to the untreated control. DS, disulfiram.

ALDH$^{high}$ cells and DTPs use specific mechanisms to maintain viability under conditions of increased oxidative stress.

### Disulfiram-induced killing of drug-tolerant cells requires increased ROS

ALDH enzymes function as detoxifying agents by reducing toxic aldehydes resulting from lipid peroxidation in cells undergoing oxidative stress (34, 31). To determine whether selectively killing of drug-tolerant cells by disulfiram reflects the role of ALDH in suppressing ROS-induced DNA damage, we used the ROS scavenger, NAC (N-acetylcysteine). In PC-9 cells, erlotinib alone caused a 6-fold increase in ROS in DTPs, and an additional 3-fold ROS increase was observed in cells cotreated with erlotinib and disulfiram. Significantly, the disulfiram effect on ROS was almost completely abrogated when NAC was added (Fig. 5A). Similar results were obtained with GTL-16-derived DTPs. A small but significant increase in ROS was observed in crizotinib/disulfiram cotreated cells, and the addition of NAC caused about 75% decrease in ROS. NAC also reduced ROS in GTL-16 DTPs by about 60% but failed to reduce erlotinib-induced ROS in PC-9–derived DTPs (Fig. 5A). These results suggest that while kinase inhibitor treatment elevates ROS in kinase-addicted cancer cells, the drug-tolerant subpopulation uses ALDH to protect against ROS-mediated cell death.

We then examined DNA damage in DTPs in the presence or absence of disulfiram and NAC. We observed significantly increased DNA damage in DTPs exposed to kinase inhibitors plus disulfiram compared with kinase inhibitor alone, and the effects of disulfiram on DNA damage were abrogated by NAC (Fig. 5B). Notably, ALDH inhibition increased the turnover of some of the ALDH isoforms (Fig. 5B and Supplementary Fig. S7B). The ROS increase in cells cotreated with kinase inhibitor and disulfiram also triggered apoptosis of DTPs as revealed by increased cleaved PARP in GTL-16–derived DTPs and BimS in PC-9–derived DTPs. Consistent with the ability of NAC to suppress disulfiram-induced DNA damage, NAC cotreatment also decreased cleaved PARP and BimS (Fig. 5B). NAC is also sufficient to rescue DTPs from the lethal effects of disulfiram (Fig. 5C). Collectively, these results suggest that increased ALDH in the drug-tolerant subpopulation maintains sufficiently low levels of ROS to prevent apoptosis.

### ALDH inhibition delays tumor relapse in xenograft mouse models

To investigate the ability of disulfiram to delay tumor relapse *in vivo*, we used a PC-9 xenograft model. The treatment regimen was first tested *in vitro*; thus, cells were treated with either erlotinib or disulfiram alone or in combination, and after 6 days, cells were maintained with or without disulfiram for four more days. We observed a significant growth delay in cells treated with erlotinib + disulfiram compared with erlotinib alone, and a further delay in erlotinib + disulfiram–treated cells that continued to receive disulfiram (Fig. 6A). A pharmacodynamic study of

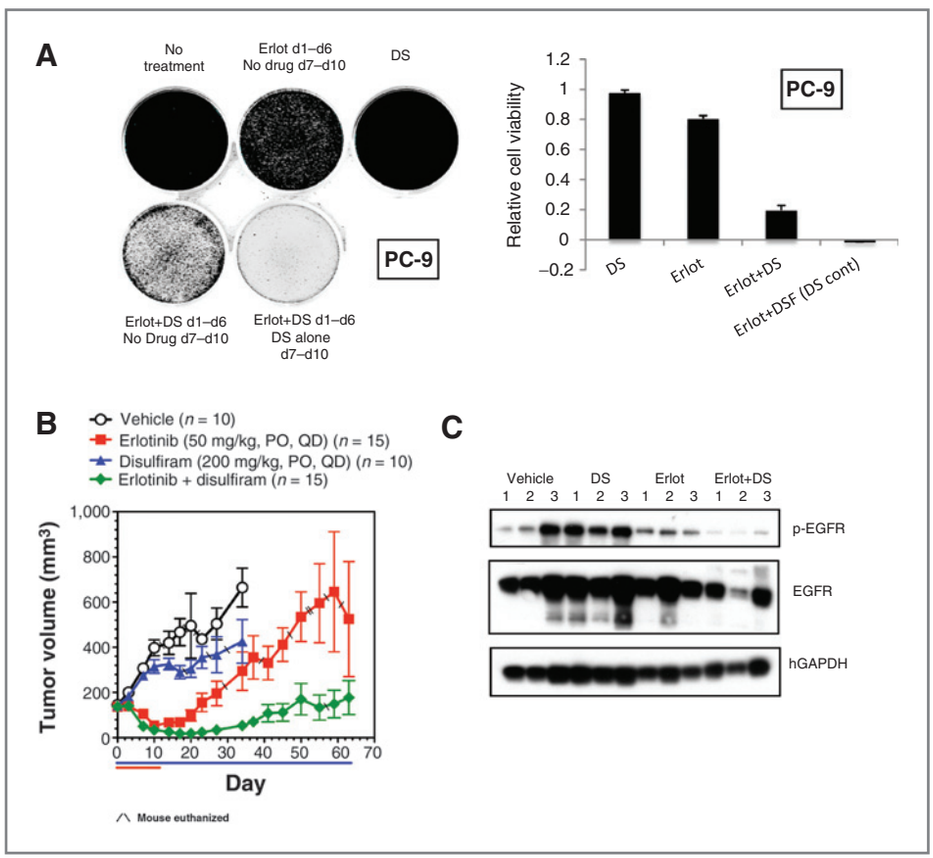


Figure 6. Disulfiram delays tumor relapse associated with acquired drug resistance. A, PC-9 parental cells were treated with erlotinib (1 μmol/L) alone or in combination with disulfiram (DS; 200 nmol/L) for 6 days, and the DTPs were then allowed to grow in erlotinib-free growth media, with or without disulfiram, for four more days (d7–d10). The bar graph reflects the quantitative measurements of the effect of disulfiram on PC-9–derived DTPs from triplicate wells. The error bars reflect SEM values. B, *in vivo* data demonstrating a significant delay in tumor relapse in disulfiram-treated PC-9 xenografts. Mice (numbers per group are indicated in the legend) were treated with erlotinib for 11 days; however, disulfiram treatment was continued in the erlotinib + disulfiram–treated animals until the end of the experiment. Group mean tumor volume with SEM is plotted. C, pharmacodynamic data illustrating the effect of erlotinib and erlotinib + disulfiram treatments on phospho-EGFR levels in xenograft tumors. DS, disulfiram.

treated tumors indicated decreased p-EGFR in both erlotinib and erlotinib + disulfiram–treated tumors (Fig. 6C).

In the xenograft tumor growth study, mice were divided into four groups, namely, vehicle control, disulfiram control, erlotinib alone, and erlotinib + disulfiram groups. As expected, erlotinib was highly effective, whereas single-agent disulfiram caused minimal efficacy (Fig. 6B and Supplementary Table S2). After 11 days of erlotinib alone or in combination with disulfiram, most tumors were substantially reduced. Therefore, to assess the added effect of disulfiram, all treatments were stopped, except for disulfiram, which was continued until the end of the study. No significant loss in body weight was observed in mice as a result of any of the treatments (Supplementary Table S2).

We observed near-complete regression of tumors with erlotinib with 11 of 15 mice responding [10 PRs (defined by >50% decrease in tumor volume) and 1 CR (no measurable tumor)]. Tumors quickly rebounded following treatment cessation, with a mean TTP of 41 days to reach twice the starting tumor volume (Supplementary Table S2). Treatment with erlotinib + disulfiram was more effective, with 15 of 15 animals responding (9 PRs and 6 CRs). Significantly, the combination treatment resulted in a prolonged response, with tumors not progressing beyond the initial tumor volume (Supplementary Table S2). These data indicate a highly significant ($P < 0.0007$) delay in tumor relapse in the erlotinib + disulfiram–treated mice compared with those treated with erlotinib alone, consistent with a role for ALDH in drug tolerance in tumors.

## Discussion

We have described a drug tolerance mechanism associated with a cancer cell subpopulation derived from various tissues of origin, which involves the ALDH enzyme family. Our observations highlight similar properties of $ALDH^{high}$ CSCs and drug-tolerant cancer cells, consistent with previously reported findings supporting a role for CSCs in drug resistance (4–6). These observations suggest potential benefit of combining ALDH inhibition with targeted cancer therapeutics as a strategy to prevent or delay cancer relapse.

Our studies initially focused on the CSC marker, *ALDH1A1*, which is enriched in a subpopulation of MET-addicted gastric cancer cells that display crizotinib tolerance. This difference in crizotinib sensitivity between $ALDH^{high}$ and $ALDH^{low}$ gastric carcinoma cells perhaps provides a mechanism by which CSCs can maintain viability upon an initial onslaught of a cytotoxic drug. The observed crizotinib-induced ALDH expression in $ALDH^{high}$ cells may provide a survival advantage over $ALDH^{low}$ cells during prolonged drug exposure. Significantly, we observed disulfiram sensitivity among DTPs derived from many cell line models, regardless of whether they specifically expressed elevated levels of the *ALDH1A1* isoform. Indeed, we observed consistently increased expression of multiple ALDH family members in drug-tolerant cells, pointing to the effectiveness of disulfiram in inhibiting multiple ALDH isoforms. Our results are consistent with the previous observation that simultaneous knockdown of two ALDH members results in increased cyclophosphamide sensitivity of lung cancer cells compared with knockdown of individual members (35). These findings may explain why *ALDH1A1* alone, as a prognostic biomarker for worse clinical outcome and metastasis in cancer, has at best, yielded mixed results (20). In metastatic breast cancer, such a correlation improved significantly when expression of *ALDH1A3*, *ALDH2*, and *ALDH6A1* isoforms, as well as *ALDH1A1*, was considered (36). Together, these results point to a likely role for multiple ALDH family members in drug resistance.

The ALDH requirement in drug-tolerant cells for survival under prolonged drug exposure implicates a drug-induced increase in aldehyde levels. We speculate that increased oxidative stress in drug-tolerant cells, leading to membrane lipid peroxidation, is a likely cause of increased aldehyde levels. The observed increased dependence on mitochondrial respiration,

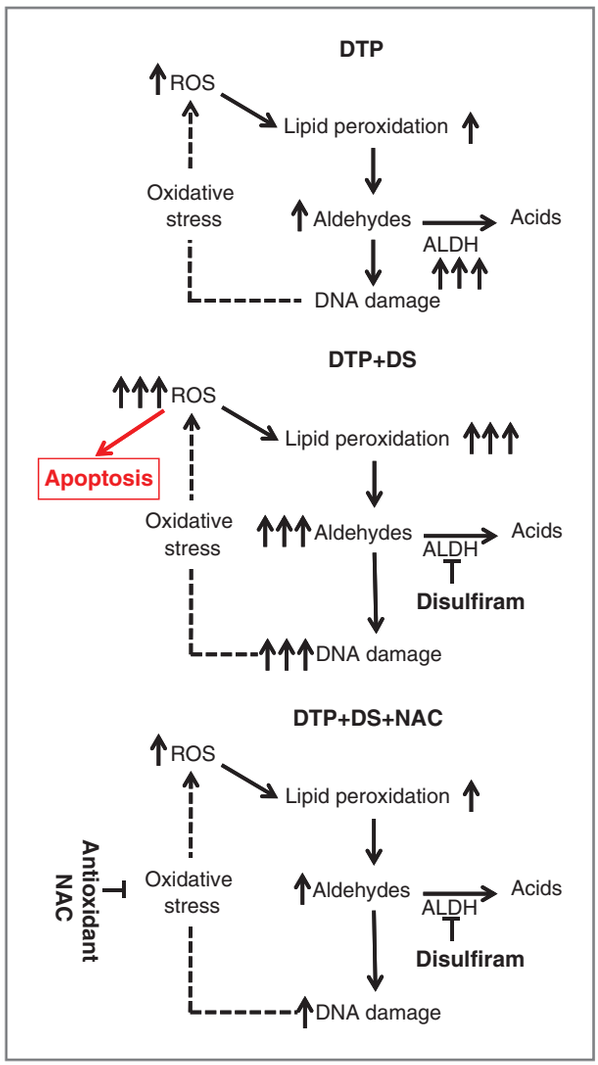


Figure 7. Models depicting the proposed mechanism underlying the specific cytotoxic effect of disulfiram (DS) on DTPs. Accumulation of toxic aldehydes in kinase inhibitor–treated cancer cells increases ROS levels particularly in the drug-tolerant population. ALDH activity is required to maintain ROS levels sufficiently low to prevent triggering of apoptosis. Inhibition of ALDH activity by disulfiram increases ROS levels above a threshold, consequently triggering apoptosis, a process that can be suppressed by the ROS scavenger NAC.

measured as increased OCR/ECAR ratio, is probably a major source of increased ROS in drug-tolerant cells. Interestingly, CSCs identified from gastric cancer cells, defined by high ALDH1A1 expression, also exhibit elevated ROS and increased OCR/ECAR, similar to what is seen in the drug-tolerant cells, and further supporting the presence of a subpopulation of preexisting (before treatment) cancer cells that exhibit characteristics of drug-tolerant cells.

One of the major consequences of increased oxidative stress levels is the accumulation of DNA lesions, which can lead to apoptosis. The activation of DDR in glioma-derived CSCs at a level higher than that seen in non-CSCs may contribute to the observed resistance to ionizing radiotherapy (10). Similarly, we detected increased double-stranded DNA breaks in our model systems, suggesting that activation of DDR may be a widely used mechanism of survival of a subpopulation of cancer cells during cancer therapy.

Other reported mechanisms of action of disulfiram, including inhibition of P-glycoproteins involved in drug efflux and proteasome inhibition, are seen at relatively higher disulfiram concentrations (37, 38). However, our findings indicating complete inhibition of phospho-MET in MKN-45 and GTL-16 DTPs (Supplementary Fig. S9A) by crizotinib (even in the presence of disulfiram), together with no apparent effect of a proteasome inhibitor MG132 on DTP formation (Supplementary Fig. S9B), would seem to exclude these alternative potential mechanisms of disulfiram action on DTPs. A recent study of paclitaxel-resistant MDA-MB-231 cells (39) demonstrated cytotoxic effect of disulfiram/$Cu^{++}$ on the resistant cells; however, in contrast to our observation of a lethal effect of disulfiram specific to drug-tolerant cells, disulfiram/$Cu^{++}$ was equally toxic to parental MDA-MB-231 cells.

We propose a model (Fig. 7) implicating ALDH family members in maintaining intracellular aldehyde levels (and consequently, ROS levels) below the threshold beyond which an apoptotic response is engaged. Our findings with NAC cotreatment emphasize the critical importance of managing ROS levels for the survival of drug-tolerant cells and raise the possibility of discovering additional therapeutics that can specifically elevate ROS levels within the drug-tolerant cells to delay tumor relapse. Notably, NAC does not protect drug-sensitive cells from the lethal effects of targeted therapies, consistent with a unique role in the CSC-like subpopulation.

Our *in vivo* findings demonstrate a beneficial effect of the combination of disulfiram and erlotinib in significantly delaying treatment relapse. Significantly, a phase II clinical trial performed almost two decades ago demonstrated an increased survival rate of patients with breast cancer who received chemotherapy plus an active disulfiram metabolite compared with chemotherapy alone (40). Altogether, these observations suggest a potential benefit of ALDH inhibition for the treatment of breast and other cancers. If the cell culture findings with disulfiram cotreatment can be similarly translated to the clinic, there may be broad opportunities to use this therapeutic strategy to delay tumor relapse in various cancer treatment contexts.

## Disclosure of Potential Conflicts of Interest

M. Merchant is employed with Genentech and Roche as Sr. Scientist and has ownership interest (including patents) with Roche. J. Settleman has other commercial research support from Genentech. No potential conflicts of interest were disclosed by the other authors.

## Authors' Contributions

**Conception and design:** D. Raha, T.R. Wilson, J. Settleman
**Development of methodology:** D. Raha, J. Peng, D. Peterson
**Acquisition of data (provided animals, acquired and managed patients, provided facilities, etc.):** D. Raha, J. Peng, D. Peterson, M. Merchant
**Analysis and interpretation of data (e.g., statistical analysis, biostatistics, computational analysis):** D. Raha, T.R. Wilson, J. Peng, D. Peterson, P. Yue, M. Evangelista, M. Merchant, J. Settleman
**Writing, review, and or revision of the manuscript:** D. Raha, T.R. Wilson, M. Evangelista, M. Merchant, J. Settleman
**Study supervision:** M. Evangelista, M. Merchant, J. Settleman
**Performed laboratory experiments:** C. Wilson

## Acknowledgments

The authors thank members of Settleman Laboratory, especially Ho-June Lee, for helpful discussions, R. Soriano and G. Fedorowicz for microarray services, the Genentech Laboratory Animal Resource, and the gCELL and FACS core laboratories for support.

## Grant Support

This work was supported by Genentech, Inc., a member of the Roche group.

The costs of publication of this article were defrayed in part by the payment of page charges. This article must therefore be hereby marked *advertisement* in accordance with 18 U.S.C. Section 1734 solely to indicate this fact.

Received December 4, 2013; revised March 16, 2014; accepted March 29, 2014; published OnlineFirst May 8, 2014.

## References

1. Torti D, Trusolino L. Oncogene addiction as a foundational rationale for targeted anti-cancer therapy: promises and perils. EMBO Mol Med 2011;3:623–36.
2. Sharma SV, Settleman J. Oncogene addiction: setting the stage for molecularly targeted cancer therapy. Genes Dev 2007;21:3214–31.
3. Weinstein IB. Cancer. Addiction to oncogenes-the Achilles heal of cancer. Science 2002;297:63–64.
4. Singh A, Settleman J. EMT, Cancer stem cells and drug resistance: an emerging axis of evil in the war on cancer. Oncogene 2010;29:4741–51.
5. Dean M, Fojo T, Bates S. Tumour stem cells and drug resistance. Nat Rev Cancer 2005;5:275–84.
6. Holohan C, Schaeybroeck SV, Longley DB, Johnston PG. Cancer drug resistance: an evolving paradigm. Nat Rev Cancer 2013;10:714–26.
7. Szatrowski TP, Nathan CF. Production of large amounts of hydrogen peroxide by human tumor cells. Cancer Res 1991;51:794–8.
8. Zhou Y, Hileman EO, Plunkett W, Keating MJ, Huang P. Free radical stress in chronic lymphocytic leukemia cells and its role in cellular sensitivity to ROS-generating anticancer agents. Blood 2003;101:4098–104.
9. Kumar B, Koul S, Khandrika L, Meacham RB, Koul HK. Oxidative stress is inherent in prostate cancer cells and is required for aggressive phenotype. Cancer Res 2008;68:1777–85.
10. Bao S, Wu Q, McLendon RE, Hao Y, Shi Q, Hjelmeland AB, et al. Glioma stem cells promote radioresistance by preferential activation of the DNA damage response. Nature 2006;444:756–60.
11. Diehn M, Cho RW, Lobo NA, Kalisky T, Dorie MJ, Kulp AN, et al. Association of reactive oxygen species levels and radioresistance in cancer stem cells. Nature 2009;458:780–3.

12. Schmitt CA, Lowe SW. Bcl-2 mediates chemoresistance in matched pairs of primary E(mu)-myc lymphomas *in vivo*. Blood Cells Mol Dis 2001;27:206–16.
13. Yeung J, Esposito MT, Gandillet A, Zeisig BB, Griessinger E, Bonnet D, et al. $\beta$-Catenin mediates the establishment and drug resistance of MLL leukemic stem cells. Cancer Cell 2010;18:606–18.
14. Domingo-Domenech J, Vidal SJ, Rodriguez-Bravo V, Castillo-Martin M, Quinn SA, Rodriguez-Barrueco R, et al. Suppression of acquired docetaxel resistance in prostate cancer through depletion of notch- and hedgehog-dependent tumor-initiating cells. Cancer Cell 2012;22: 373–88.
15. Zhang Q, Shi S, Yen Y, Brown J, Ta JQ, Le AD. A subpopulation of CD133(+) cancer stem-like cells characterized in human oral squamous cell carcinoma confer resistance to chemotherapy. Cancer Lett 2010;289:151–60.
16. Auvinen P, Tammi R, Tammi M, Johansson R, Kosma VM. Expression of CD 44 s, CD 44 v 3 and CD 44 v 6 in benign and malignant breast lesions: correlation and colocalization with hyaluronan. Histopathology 2005;4:420–8.
17. Ginestier C, Hur MH, Charafe-Jauffret E, Monville F, Dutcher J, Brown M, et al. ALDH1 is a marker of normal and malignant human mammary stem cells and a predictor of poor clinical outcome. Cell Stem Cell 2007;1:555–67.
18. Bourguignon LY, Peyrollier K, Xia W, Gilad E. Hyaluronan-CD44 interaction activates stem cell marker Nanog, Stat-3-mediated MDR1 gene expression, and ankyrin-regulated multidrug efflux in breast and ovarian tumor cells. J Biol Chem 2008;283:17635–51.
19. Keysar SB, Jimeno A. More than markers: biological significance of cancer stem cell-defining molecules. Mol Cancer Ther 2010;9:2450–7.
20. Marcato P, Dean CA, Giacomantonio CA, Lee PW. Aldehyde dehydrogenase: its role as a cancer stem cell marker comes down to the specific isoform. Cell Cycle 2011;10:1378–84.
21. Tanei T, Morimoto K, Shimazu K, Kim SJ, Tanji Y, Taguchi T, et al. Association of breast cancer stem cells identified by aldehyde dehydrogenase 1 expression with resistance to sequential Paclitaxel and epirubicin-based chemotherapy for breast cancers. Clin Cancer Res 2009;15:4234–41.
22. Sharma SV, Lee DY, Li B, Quinlan MP, Takahashi F, Maheswaran S , et al. A chromatin-mediated reversible drug tolerant state in cancer cell subpopulations. Cell 2010;141:69–80.
23. Wilson TR, Lee DY, Berry L, Shames DS, Settleman, J. Neuregulin-1-mediated autocrine signaling underlies sensitivity to HER2 kinase inhibitors in a subset of human cancers. Cancer Cell 2011;20:158–72.
24. Pinheiro J, Bates D, DebRoy S, Sarkar Dand R Core Team. nlme: linear and nonlinear mixed effects models. R package, version 3.1 96; 2014. Available from: http://cran.r-project.org/package=nlme.
25. R Development Core Team. R: a language and environment for statistical computing. Vienna, Austria: R Foundation for Statistical Computing; 2008. ISBN 3 900051 07 0. Available from: http://www.R project.org.
26. Storms RW, Trujillo AP, Springer JB, Shah L, Colvin OM, Ludeman SM, et al.Isolation of primitive human hematopoietic progenitors on the basis of aldehyde dehydrogenase activity. Proc Natl Acad Sci U S A 1999;96:9118–9123.
27. Levi BP, Yilmaz OH, Duester G, Morrison SJ. Aldehyde dehydrogenase 1a1 is dispensable for stem cell function in the mouse hematopoietic and nervous systems. Blood 2009;113:1670–80.
28. Moore SA, Baker HM, Blythe TJ, Kitson KE, Kitson TM, Baker EN. Sheep liver cytosolic aldehyde dehydrogenase: the structure reveals the basis for the retinal specificity of class 1 aldehyde dehydrogenases. Structure 1998;6:1541–51.
29. Koppaka V, Thompson DC, Chen Y, Ellermann M, Nicolaou KC, Juvonen RO , et al. Aldehyde dehydrogenase inhibitors: a comprehensive review of the pharmacology, mechanism of action, substrate specificity, and clinical application. Pharmacol Rev 2012;64:520–39.
30. Rekha GK, Sladek NE. Inhibition of human class 3 aldehyde dehydrogenase, and sensitization of tumor cells that express significant amounts of this enzyme to oxazaphosphorines, by the naturally occurring compound gossypol. Adv Exp Med Biol 1997;414:133–46.
31. Barrera G. Oxidative stress and lipid peroxidation products in cancer progression and therapy. ISRN Oncol 2012;2012:1–21.
32. Choi J, Liu RM, Forman HJ. Adaptation to oxidative stress: quinone-mediated protection of signaling in rat lung epithelial L2 cells. Biochem Pharmacol 1997;53:987–93.
33. Blanpain C, Mohrin M, Sotiropoulou PA, Passegué E. DNA-damage response in tissue-specific and cancer stem cells. Cell Stem Cell 2011;8:16–29.
34. Singh S, Brocker C, Koppaka V, Chen Y, Jackson BC, Matsumoto A, et al. Aldehyde dehydrogenases in cellular responses to oxidative/electrophilic stress. Free Radic Biol Med 2013;56:89–101.
35. Moreb JS, Mohuczy D, Ostmark B, Zucali JR. RNAi-mediated knockdown of aldehyde dehydrogenase class-1A1 and class-3A1 is specific and reveals that each contributes equally to the resistance against 4-hydroperoxycyclophosphamide. Cancer Chemother Pharmacol 2007; 59:127–36.
36. Marcato P, Dean CA, Pan D, Araslanova R, Gillis M, Joshi M , et al. Aldehyde dehydrogenase activity of breast cancer stem cells is primarily due to isoform ALDH1A3 and its expression is predictive of metastasis. Stem Cells 2011;29:32–45.
37. Sauna ZE, Peng X-H, Nandigama K, Tekle S, Ambudkar SV. The molecular basis of the action of disulfiram as a modulator of the multidrug resistance-linked ATP binding cassette transporters MDR1 (ABCB1) and MRP1 (ABCC1). Mol Pharmacol 2004;65:675–684.
38. Chen D, Cui QC, Yang H, Dou QP. Disulfiram, a clinically used anti-alcoholism drug and copper-binding agent, induces apoptotic cell death in breast cancer cultures and xenografts via inhibition of the proteasome activity. Cancer Res 2006;66:10425–10433.
39. Liu P, Kumar IS, Brown S, Kannappan V, Tawari PE, Tang JZ, et al. Disulfiram targets cancer stem-like cells and reverses resistance and cross-resistance in acquired paclitaxel-resistant triple-negative breast cancer cells. Br J Cancer 2013;109:1876–1885.
40. Dufour P, Lang JM, Giron C, Duclos B, Haehnel P, Jaeck D, et al. Sodium dithiocarb as adjuvant immunotherapy for high risk breast cancer: a randomized study. Biotherapy 1993;6:9–12.